Synthesis of dye conjugates to visualize the cancer cells using fluorescence microscopy

Yang Pu,[1] Rui Tang,[2] Jianpeng Xue,[2,3] W. B. Wang,[1] Baogang Xu,[2] and S. Achilefu[2,*]

[1]Department of Physics at the City College of the City University of New York,
160 Convent Avenue, New York, New York 10031, USA

[2]Department of Radiology, Washington University in St. Louis, School of Medicine,
4525 Scott Avenue, St. Louis, Missouri 63110, USA

[3]Department of Biomedical Engineering, China Pharmaceutical University, Nanjing 210009, China

*Corresponding author: achilefus@mir.wustl.edu

The clinical diagnosis of most cancers is based on evaluation of histology microscopic slides to view the size and shape of cellular nuclei and morphological structure of tissue. To achieve this goal for *in vivo* and in-deep tissues, near infrared dyes-bovine serum albumin and immunoglobulin G conjugates were synthesized. The spectral study shows that the absorption and fluorescence of the dye conjugates are in the "tissue optical window" spectral ranges between 650 and 900 nm. The internalization and pinocytosis of the synthesized compounds were investigated at cell level using fluorescence microscopy to obtain the optimal concentration and staining time.   © 2014 Optical Society of America
  OCIS codes: (000.1430) Biology and medicine; (000.2060) Education; (180.2520) Fluorescence microscopy.
  http://dx.doi.org/10.1364/AO.53.002345

1. Introduction

Optical methods can utilize low energy radiation in the near infrared (NIR) range to detect pathologic conditions and monitor the progression or retrogression of tumors [1,2]. However, until now, the confirmation of most cancers still depended on biopsy samples taken randomly from the suspected organ. Histology slides are used to diagnose the precursors and stages of cancers based on phenotypic markers, such as nuclear-to-cytoplasmic ratio and appearance of cell nuclei. The optical fluorescence microscopy technique has the potential to function as an "optical biopsy" to view these features *in vivo*. Cypate dyes are a class of nontoxic, bright, and photo-stable organic fluorophores that have shown great advantages in optical imaging. However, due to the

hydrophobic nature of cypate dyes, they are not suitable for biological applications. A carrier is required to deliver these NIR fluorophores *in vivo*. For this purpose, NIR dyes-bovine serum albumin (BSA) and immunoglobulin G (IgG) conjugates were investigated [1]. The conjugated compounds were purified on a Sephadex G-25 column with 1× phosphate-buffered saline (PBS) buffer. Fractions were evaluated using sodium dodecyl sulfate polyacrylamide gel electrophoresis (SDS-PAGE). The absorption and fluorescence spectra of the dye bioconjugates were measured and shown to be within the NIR "tissue optical window" between 650 and 900 nm. The peak positions of both absorption and fluorescence spectra of newly synthesized compounds were observed to be similar to that of corresponding free dyes. Fluorescence microscopy measurements were performed for dye-bioconjugates-stained different cell lines with outfitted far red to NIR light sources and corresponding filters for visual confirmation of

internalization and pinocytosis of the synthesized compounds in cell lines. The dye, 4′,6-diamidino-2-phenylindole (DAPI), was used to stain cell nuclei [3]. The time and concentration dependences of cell staining of the compounds were systematically studied to obtain the optimal concentration and staining time. This study serves as a step to forward to our *in vivo* histological microscopy evaluation using "optical biopsy" and illustrates the protocol for synthesis of dye-bioconjugates using the efficient two-step coupling of protein with the dye [3]. It can be used as a helpful tutorial or note for researchers in the field of biomedical optics to know how to design, develop, synthesize, and test dye-bioconjugates working as optical contrast agents for cancer detection.

2. Methods and Samples

A. ICG, Cypate, and Cypate 3

Indocyanine Green (ICG), also called Cardio-Green, is the only U.S. Food and Drug Administration (FDA)-approved clinical dye in the NIR range. It is one of the most important cyanine dyes since its fluorescence is in the spectral range between 775 and 850 nm, existing in the NIR "tissue optical window." The molecular structure of ICG is schematically shown in Fig. 1(a).
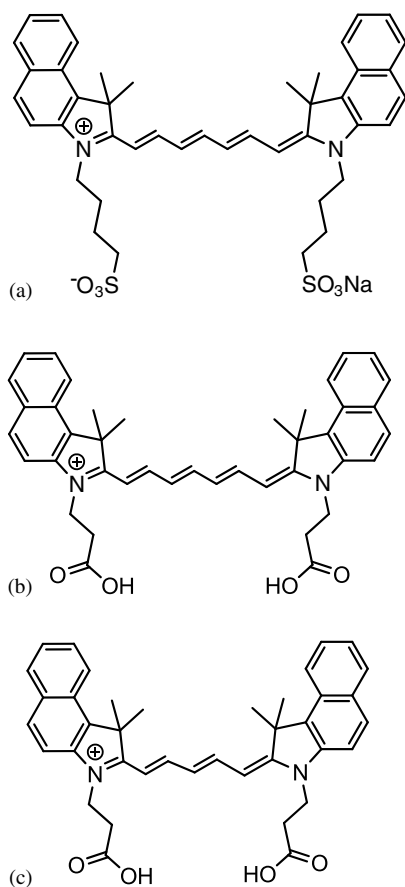

Fig. 1. Molecular structure of (a) ICG, (b) dye cypate, and (c) dye cypate 3.

Cypate dye (1H-Benz[e]indolium, 3-(2-carboxyethyl)-2-[7-[3-(2-carboxyethyl)-1,3-dihydro-1,1-dimethyl-2H-benz[e]indol-2-ylidene]-1,3,5-heptatrienyl]-1,1-dimethyl-,chloride) and cypate 3 dye (1H-Benz[e]indolium, 3-(2-carboxyethyl)-2-[7-[3-(2-carboxyethyl)-1,3-dihydro-1,1-dimethyl-2H-benz[e]indol-2-ylidene]-1,3-pentadienyl]-1,1-dimethyl-,chloride) are ICG-derivative NIR dyes. Cypate and cypate 3 dyes used in this study were prepared with the expertise of biochemistry at Achilefu's group at the Washington University School of Medicine. The synthesis of this type of contrast agent was reported elsewhere [1]. The molecular structures of cypate and cypate 3 are shown in Figs. 1(b) and 1(c), respectively. The major difference between the cypate and cypate 3 structures is the length of their trans-chain. Compared with the clinically used dye, ICG, the main advantage of the studied cypate or cypate 3 dyes is their carboxylic group. Usually an antibody or peptide has an amino group, which can be conjugated with the carboxylic group of cypate/cypate 3 to form an amide bond. This property makes cypate and cypate 3 better than other NIR dyes since they can be easily engineered to prepare a library of ligands (peptides or antibodies) for rapid identification of bioactive molecules [1]. Another advantage of the cypate family is its preservation of the absorption and fluorescence spectra in the NIR "tissue optical window" [2]. The difference of cypate and cypate 3 in the length of their polymethane chains makes their absorption and emission peaks different from each other.

B. Materials

The 2-(N-morpholino) ethanesulfonic acid (MES) and NaCl with pH 6.0 were used as activation buffer. 1-ethyl-3-(3-dimethylaminopropyl) carbodiimide (EDC) and N-hydroxysulfosuccinimide (Sulfo-NHS) were used as buffers throughout the study. Bovine serum albumin (BSA, grade agarose gel electrophoresis, 99%) and immunoglobulin G (IgG) were purchased from commercial sources. BSA and/or IgG were selected for the conjugation of cypate dye because these proteins have shown advantages in bringing hydrophobic dyes into aqueous environments to help both circulating time and internalization in comparison with polymers [4]. The polyethylene glycol (PEG)-conjugated hydrophobic dyes may form self-assembled micelle, and the size and properties of the micelle are hard to be controlled and predicted. The conjugates of BSA-dye cypate and cypate 3, IgG-dye cypate and cypate 3 were synthesized, purified, and characterized.

C. Synthesis

1. BSA-cypate conjugation:

We apply a protocol adapted from the method of Zhao *et al.* [3], which is efficient two-step coupling of protein and dye using EDC and sulfo-NHS. The presence of Sulfo-NHS stabilizes the amine-reactive intermediate by converting it to an amine-reactive

Sulfo-NHS ester, thus increasing the efficiency of EDC-mediated coupling reactions.

The steps of the adapted conjugation protocol are as follows [3]:

(a) 0.0021 mol (0.4 mg) EDC and 1 mg (0.0046 mol) Sulfo-NHS were added in 1 ml activation buffer: 0.1 M MES, 0.5 M NaCl, pH 6.0;

(b) 0.0016–0.0032 mol (1–2 mg) cypate was added in the reaction mixture and shaken at room temperature for 0.5–1 hours;

(c) 0.54 mmol (36 mg) BSA was dissolved in reaction mixture generated by steps 1 and 2, and shaken at room temperature for overnight; and

(d) The conjugate was purified on a Sephadex G-25 column with the MES buffer.

The labeling efficiencies between the selected dyes and proteins were evaluated via UV/Vis absorption measurements for the conjugates in the 1X PBS buffer analyzed using a standard equation [5] and were found to be ~0.82 for dye/BSA, mol/mol, and ~1.1 for dye/IgG, mol/mol.

2. IgG–cypate, BSA–cypate 3, and IgG–cypate 3 conjugations:

A similar protocol is applied in these conjugations. While one certain conjugation procedure was performed, either cypate or cypate 3 and either BSA or IgG were added together to form the dye conjugates. The reason for using BSA and IgG is to minimize the aggregation of the hydrophobic dye in biological systems. Aggregation of the dye will cause the change of absorption spectra (J- and H-aggregates) and the self-quenching of the fluorescence [6]. Using the protein conjugated cypate dye family can bring these hydrophobic dyes to the targeted hydrophilic dye level in imaging studies.

D. Cell Culture

The primary tumor carcinoma (MCF-7) [7], moderate metastatic (DU-145) [8], and advanced metastatic (PC-3) [8] cell lines were purchased from ATCC (Manassas, Va.) and stored in the condition of 95% air-5% CO_2 at 37°C. The primary breast cancer MCF-7 cells were cultured in Dulbecco's minimum essential medium (DMEM; Sigma Chemical Co., St. Louis, Missouri) with 10% fetal bovine serum (FBS; Gibco BRL, Cleveland, Ohio), 100 U penicillin, 0.1 μg streptomycin, and 2 mmol/l L-glutamax in a humidified incubator maintained at 37°C with 5% CO_2. The moderate metastatic prostate DU-145 cells were cultured in Minimum Essential Medium Eagle (MEM; Sigma Chemical Co., St. Louis, Missouri, USA) with 10% fetal bovine serum (FBS; Gibco BRL, Cleveland, Ohio), 2 mM L-Glutamin, 1.5 g/L Na-bicarbonate, 4.5 g/L glucose, 0.1 mM NEAA, and 1.0 mM Na-pyruvate. The advanced metastatic PC-3 cell lines cultured in Ham's F-12 K medium (Life Technologies, Carlsbad, California) were supplemented with 20% fetal bovine serum (FBS; Gibco

BRL, Cleveland, Ohio), 1.5 g/l $NaHCO_3$, 1.5 g/l sodium, and 2 mM L-glutamine. On harvesting days, which varied depending on different cell lines, the cells were harvested by treatment with Trypsin-EDTA (5% trypsin and 5.3×10^{-6} M EDTA: GIBCO) for 5–10 min, diluted in the medium, then isolated by centrifugation. They were resuspended in PBS provided by SIGMA to be washed [9]. The cells (1×10^5 cells/well) were then grown on LabTek 8-chamber slides (Nunc Inc. Rochester, New York) overnight prior to the experiments. For the optimal staining time study, all compounds were dissolved in 20% aqueous DMSO and diluted in 0.01 M PBS (pH 7.4) (Sigma, St. Louis) to a concentration of 10 μM. Each compound (10 μM) was added to the cells in chambers to obtain final concentration of 1 μM and incubated at 37°C or 4°C. The samples were analyzed at different time points [9]. For the concentration dependence study, cells were incubated in compounds with different concentrations for ~4 hours at 37°C. After washing four times with 0.01 M PBS (pH 7.4), the cells were stained for 2–3 min with fluorescence agent DAPI for visual nuclei at room temperature. Cells were covered with coverslips and sealed with nail polish. An Olympus fluorescence microscope (BX 51) was used to analyze all samples.

3. Experimental Results and Discussion

A. Confirmation of the Conjugation Using SDS-PAGE

An activated carboxylic group of cypate and cypate 3 was conjugated with BSA and/or IgG. The conjugation of cypate and cypate 3 to proteins was confirmed by SDS-PAGE. As an example, the fluorescence image of cypate 3 SDS-PAGE for cypate 3-protein conjugates gel was obtained using a small animal imaging system, Pearl Imager (Li-COR), and is shown in Fig. 2. Both lanes 1 and 7 are fluorescent ladders, which are used to index molecular weight (MW) of the compound. The lanes 2 and 3 were loaded with unconjugated cypate 3. The cypate 3-protein conjugates with different concentrations were loaded in
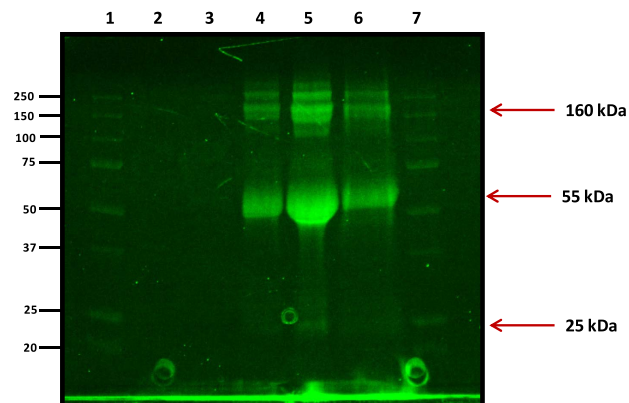

Fig. 2. SDS-PAGE of cypate 3-protein conjugates. Lanes 1 and 7 for fluorescent ladder, lanes 2 and 3 for unconjugated cypate 3, and lanes 4, 5, and 6 for cypte 3-protein conjugates with different concentrations.

lanes 4, 5, and 6. It can be seen from Fig. 2 that the free cypate 3 dye appears less than 1 kDa (at the bottom of the gel). The BSA conjugates showed bands corresponding to the appropriate MW with ~160 kDa while IgG showed bands corresponding to the heavy chain of MW with ~55 kDa [10]. A pattern often observed in the SDS-PAGE gel is usually the heavy-chain, which is a subunit of IgG protein [11].

B. Absorption and Fluorescence Spectra of Cypate 3 and Cypate Dyes and their Conjugates

Optical properties of cypate 3 and cypate dyes and their protein conjugates were investigated. The absorption and fluorescence spectral features of dye conjugates can be used as the reference for a fluorescence microscope imaging study. In our spectral study, cypate 3 and cypate conjugates were solvated in the MES and NaCl with pH 6.0 buffers. The absorption spectra of cypate and cypate 3 were measured using a Beckman Coulter DU640 UV-visible spectrophotometer in the spectral range of 300–900 nm. The absorption spectra were collected with a resolution of ~1 nm [12]. Absorption or optical density (OD) measurements can be used to determine the concentration of compounds using the Beer–Lambert law, which is known as

$$I = I_0 10^{-\varepsilon c l} = I_0 10^{-Kl}, \tag{1}$$

where ε is the molar extinction coefficient, c is the concentration, and l is the path that the light travels. The OD measurement gives light attenuation after traveling in the solution of the compound depending on the product of ε, c, and l. In our measurements, cells with thickness of 1 cm are used. Since, the molar extinction coefficient of certain compounds such as ICG, cypate 3, or cypate can be found from the previous study [13], the concentration can be obtained using the results of the OD measurements and Eq. (1). In our study, cypate 3 and cypate conjugates were diluted with 1:n to fall in the accurate measurement range of OD from 0.01 to 0.1. Once the optimal condition was satisfied, the compound solution was measured at least three times by diluting the

conjugates solution by 1:2:4. The OD values should be linearly dependent on the concentration. The measurements with different concentrations were used to reduce the error of experimental results.

The fluorescence spectra were measured using the Fluorolog-3 spectrofluorometer system provided by Jobin Yvon Inc. of Horiba Group at Edison, New Jersey. The excitation light with 5 nm spectral width was focused on samples with a spatial size of ~3 × 1 mm. The power of the incident light was ~0.5 μW. The scan speed was 200 nm/min. The fluorescence was collected with a resolution of ~1 nm.

Figures 3(a) and 3(b) show the measured absorption (dashed line) and fluorescence (solid line) spectra of cypate 3 and cypate, respectively. The absorption band of cypate 3 ranges from ~550 to 750 nm with a strong peak at 704 nm and a shoulder peak at 650 nm. The fluorescence spectrum of cypate 3 covers 680–850 nm with a main peak at 720 nm. The absorption band of cypate ranges from ~650 to 850 nm with a strong peak at 802 nm and a shoulder peak at 732 nm. The fluorescence spectrum of cypate covers from 770 to 900 nm with a main peak at 820 nm. The results show that both the cypate 3 and cypate conjugates possess the spectral advantages of the fluorescence and the absorption ranges being in the "tissue optical window" from 650 to 1100 nm. The differences of the absorption and fluorescence peaks between cypate and cypate 3 can be used to mark different NIR specific contrast agents to target different cancer receptors.

C. Determination of Dye–IgG Conjugation Internalization Using Fluorescence Microscope

The internalization of the cypate 3-IgG conjugate was investigated by using a red channel for excitation and monitoring using an Olympus BX51 WI fluorescence microscope. A 40× objective lens was used for microscopy study. The chamber slide system [8 wells, Permanox slide, 0.8 cm^2/well, sterile, 96/cs (Sigma-Aldrich)] were used for time- and concentration-dependent studies. Internalization of the compounds in cells was investigated at 0.5, 1, 2, 4, 8, 16 and 24 h incubation in live MCF-7 cells using the cypate 3-IgG conjugate with 10 μM concentrations, and the results
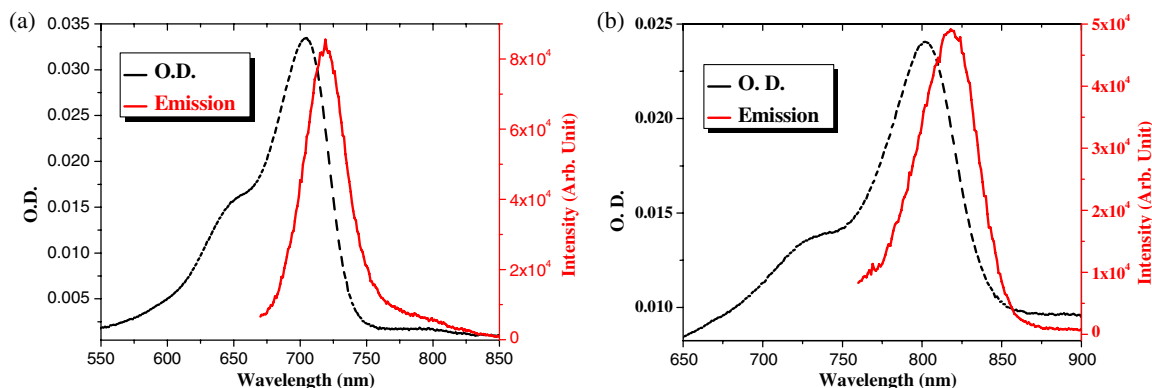

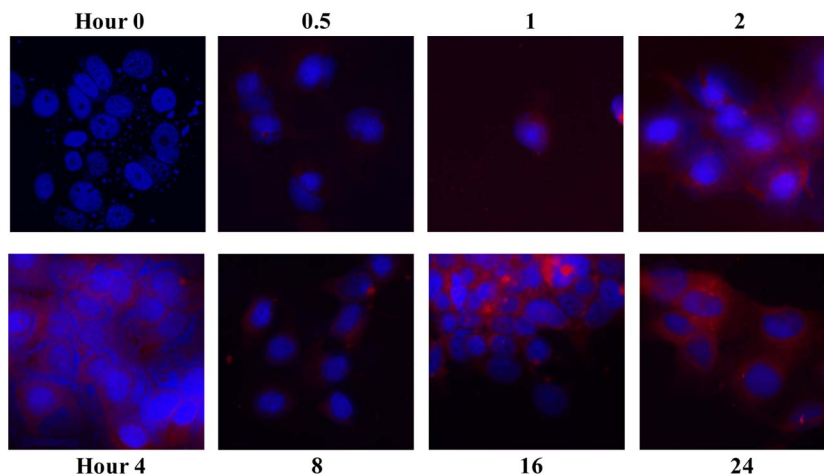Fig. 3. OD (dashed line) and fluorescence (solid line) spectra of (a) cypate 3 and (b) cypate.

Fig. 4. Intracellular distribution of 10 µM cypate 3-IgG conjugate in MCF 7 cells at 37°C at 0.5, 1, 2, 4, 8, 16, and 24 h. The nuclei stained with DAPI is shown as blue, and cells stained with cypate 3 are shown as red. The unstained control cells were indexed as hour 0.

are shown in Fig. 4. The cells incubated with a culture medium and DAPI (nuclear dye) alone in a 0.01 M PBS buffer were used as controls. The imaging parameters were kept the same for the control and sample groups. Quantification was performed by measuring fluorescence intensity in the cytoplasm at different time points. For the concentration dependence experiments, cypate-IgG conjugates with 0, 0.01, 0.05, 1, 5, 10, 25, and 50 µM concentrations were incubated in live MCF-7, DU-145, and PC3 cells lines for 8 hours. The stained cell lines were imaged with an Olympus fluorescence microscope. The mean fluorescence intensity of the cell lines was analyzed using the ImageJ software. For each image, the same analysis procedures were applied: (1) randomly choose five positions in cytoplasm to read the fluorescence intensity; (2) randomly choose five positions far from the cell as the background; (3) subtract the intensity of background from the fluorescence intensity; and (4) perform statistical analysis to obtain the mean and standard deviation values of the fluorescence intensities for different images.

To obtain the optimal concentration and staining time for internalization and pinocytosis of the synthesized compounds in PC-3 cells, the time- and concentration-dependences of cell staining were studied. As shown in Fig. 5, the control cells without the cypate 3-IgG conjugate have no fluorescence. With the time elapse, the intracellular fluorescence intensities of the cypate 3-IgG conjugate varied slightly in the first 3 h. At hour 4, dramatic increased fluorescence intensity was observed. To quantify the fluorescence intensity changes with the staining time, each of the staining cell images were obtained by averaging a number of images taken at a same time point using ImageJ analysis, and the results are shown in Fig. 5(a).

It can be seen from Fig. 5(a) that no red fluorescence can be observed without compound staining. At the first two hours, very limited compounds entered into cells. This makes the fluorescence intensity very weak with slight fluctuations, which can be shown more clearly by extending the time range from 2 to 24 h. The dramatic increase of the fluorescence intensity occurs at the fourth hour and the
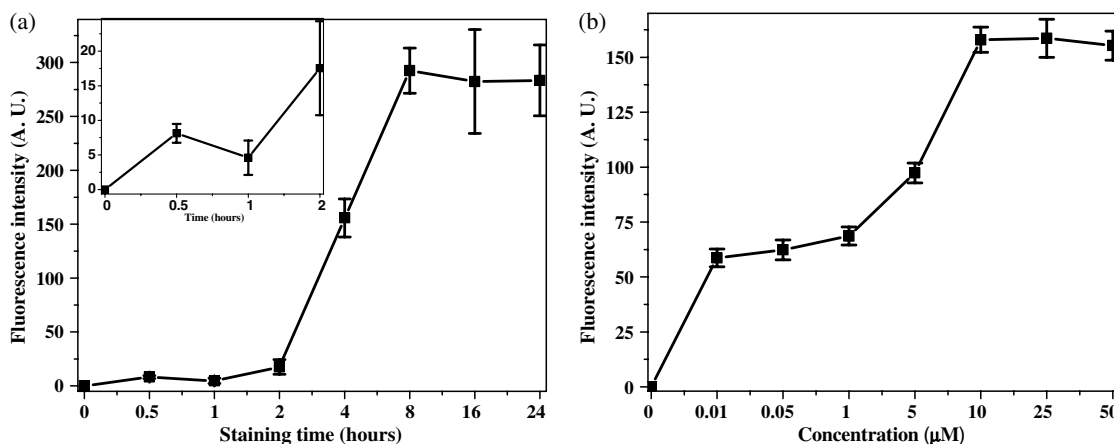

Fig. 5. (a) Staining time dependence of the synthesized cypate 3-IgG conjugate in MCF-7 cells and (b) concentration dependence of the synthesized cypate-IgG conjugate in PC-3 cells for studies of internalization and pinocytosis.

intensity keeps increasing with time until hour 8. This indicates that the most cypate 3-IgG compounds entered into the cells in the period from 4 to 8 h. From 8 to 16 h, the change of the fluorescence intensity is tiny, and shows somehow slightly decrease with a small fluctuation. The time dependence studies show that the dye–IgG compound needs ∼4 hours to enter into cell membranes. The most active time may happen within 4 to 8 h. After hour 8, the intercellular and intracellular compounds may be balanced. The pinocytosis may stop [14].

The concentration dependence studies were performed using the cypate conjugate in PC3 cell lines. Previous study shows that cypate conjugates have no obvious impact to cell viability even up to concentration of 100 μM [15]. The data were also averaged using ImageJ analysis, and the results are shown in Fig. 5(b).

No intracellular fluorescence can be observed if no cypate-IgG conjugates were added. Even when very low concentrations of 0.01 and 0.05 μM were used, obvious fluorescence can be observed. With an increase of concentration, the fluorescence intensity increases. After 10 μM, the fluorescence intensity somehow keeps unchanged with slight fluctuation. The concentration dependence studies show that the increase of the compound concentration results in an increase of fluorescence intensity, indicating a higher concentration makes more compounds enter into cell lines. The optimal concentration of dye–IgG compound is ∼10 to 25 μM.

Our study about the internalization and pinocytosis of the synthesized NIR cypate-IgG compounds may serve as the first step forward to our future *in vivo* histological microscopy evaluation using an "optical biopsy" with an NIR endoscope fiber-based probe [16]. Although there are numerous reports about optical noninvasive and/or less invasive methods for monitoring cancers, random surveillance biopsies are still the current gold standard for the identification of lesions. It was reported that the high-resolution microendoscope (HRME) developed by Richards-Kortum's group can be used to image and identify histopathologic features of metaplasia/low grade dysplasia, high grade dysplasia, and esophageal adenocarinoma [17,18]. With the help of HRME, optical biopsies will be advanced into the *in vivo* clinical stage. Optical imaging enhanced by synthesized cypate-derivative dyes combined with HRME may enable medical doctors to confirm a diagnostic conclusion because it is possible to visualize the morphological and architectural changes due to development of cancer such as the enlarged nuclear size and increased nucleus to cytoplasmic ratio *in vivo* without taking tissue samples. Furthermore, Murari *et al.* developed an all-fiber-optic scanning multiphoton endomicroscope and demonstrated two-photon (2P) imaging of cultured cells and mouse tissue, both labeled with ICG [19]. With the help of 2P endomicroscope, it is possible to not only visualize cellular feature but also benefit in reduced background fluorescence [19] and enhance the image depth in tissues [20].

4. Conclusion

In this study, the far-red dye cypate 3 and the NIR cypate-IgG conjugates were synthesized using the method of efficient two-step coupling of proteins and dyes. The conjugate was purified on a Sephadex G-25 column with 1X PBS buffer. Fractions were evaluated using SDS-PAGE. The absorption and fluorescence spectra of the dye-bioconjugates were measured and shown to exist in the NIR "tissue optical window" between 650 and 900 nm. A fluorescence microscopy study was performed for visual confirmation of internalization and pinocytosis of the synthesized compounds in MCF-7 and PC-3 cells. DAPI was used to stain cell nuclei. The time and concentration dependence of cell staining of the dye-protein conjugates were investigated. The most active time for compound internationalizing time was found within 4 to 8 h after dye-bioconjugates were added and the optimal concentration was obtained as ∼10 to 25 μM.

References

1. S. Achilefu, R. B. Dorshow, J. E. Bugaj, and R. Rajagopalan, "Novel receptor-targeted fluorescence contrast agent for *in vivo* tumor imaging," Investigat. Radiol. **35**, 479–485 (2000).
2. Y. Pu, W. B. Wang, M. Xu, G. C. Tang, Y. Budansky, M. Sharanov, S. Achilefu, J. A. Eastham, and R. R. Alfano, "Near infrared photonic finger imager for prostate cancer screening," Technol. Cancer Res. Treat. **10**, 507–517 (2011).
3. C. Zhao, Y.-L. Sun, R. L. Kirk, A. R. Thoreson, G. D. Jay, S. L. Moran, K. N. An, and P. C. Amadio, "Effects of a lubricin-containing compound on the results of flexor tendon repair in a canine model *in vivo*," J. Bone Joint Surg. Am. **92**, 1453–1461 (2010).
4. L. C. Zanetti-Domingues, C. J. Tynan, D. J. Rolfe, D. T. Clarke, and M. Martin-Fernandez, "Hydrophobic fluorescent probes introduce artifacts into single molecule tracking experiments due to non-specific binding," PLoS One **8**, e74200 (2013).
5. K. C. Black, N. D. Kirkpatrick, T. S. Troutman, L. Xu, J. Vagner, R. J. Gillies, J. K. Barton, U. Utzinger, and M. Romanowski, "Gold nanorods targeted to δ opioid receptor: plasmon-resonant contrast and photothermal agents," Mol. Imag. **7**, 50–57 (2008).
6. S. Gadde, E. K. Batchelor, and A. E. Kaifer, "Controlling the formation of cyanine dye H- and J-aggregates with cucurbituril hosts in the presence of anionic polyelectrolytes," Chemistry **15**, 6025–6031 (2009).
7. M. Uchino, H. Kojima, K. W. Mika Imada, F. Onoda, H. Satofuka, T. Utsugi, and Y. Murakami, "Nuclear b-catenin and CD44 upregulation characterize invasive cell populations

in non-aggressive MCF-7 breast cancer cells," BMC Cancer **10**, 414 (2012).

8. R. E. Sobel and M. D. Sadar, "Cell lines used in prostate cancer research: a compendium of old and new lines—part 2," J. Urol. **173**, 360–372 (2005).

9. D. Shen, K. Liang, Y. Ye, E. Tetteh, and S. Achilefu, "Modulation of nuclear internalization of Tat peptides by fluorescent dyes and receptor-avid peptides," FEBS Lett. **581**, 1793–1799 (2007).

10. J. S. Navratil, S. C. Watkins, J. J. Wisnieski, and J. M. Ahearn, "The globular heads of C1q specifically recognize surface blebs of apoptotic vascular endothelial cells," J. Immunol. **166**, 3231–3239 (2001).

11. N. Aoki, K. Furukawa, K. Iwatsuki, A. Noda, T. Sato, R. Nakamura, and T. Matsuda, "A bovine IgG heavy chain contains N-acetylgalactosaminylated N-linked sugar chains," Biochem. Biophys. Res. Commun. **210**, 275–280 (1995).

12. Y. Pu, W. B. Wang, and R. R. Alfano, "Optical detection of meat spoilage using Fluorescence spectroscopy with selective excitation wavelength," Appl. Spectrosc. **67**, 210–213 (2013).

13. M. Y. Berezin, H. Lee, W. Akers, and S. Achilefu, "Near infrared dyes as lifetime solvatochromic probes for micropolarity measurements of biological systems," Biophys. J. **93**, 2892–2899 (2007).

14. S. Achilefu, S. Bloch, M. A. Markiewicz, T. Zhong, Y. Ye, R. B. Dorshow, B. Chance, and K. Liang, "Synergistic effects of light-emitting probes and peptides for targeting and monitoring integrin expression," Proc. Natl. Acad. Sci. USA **102**, 7976–7981 (2005).

15. A. El-Faham and F. Albericio, "Peptide coupling reagents, more than a letter soup," Chem. Rev. **111**, 6557–6602 (2011).

16. Y. Pu, W. Wang, M. Xu, J. Eastham, G. Tang, and R. R. Alfano, "Characterization and three-dimensional localization of cancerous prostate tissue using backscattering scanning polarization imaging and independent component analysis," J. Biomed. Opt. **17**, 081419 (2012).

17. D. Shin, M. C. Pierce, A. M. Gillenwater, M. D. Williams, and R. R. Richards-Kortum, "A fiber-optic fluorescence microscope using a consumer-grade digital camera for in vivo cellular imaging," PLoS One **5**, e11218 (2010).

18. T. J. Muldoon, N. Thekkek, D. Roblyer, D. Maru, N. Harpaz, J. Potack, S. Anandasabapathy, and R. R. Richards-Kortum, "Evaluation of quantitative image analysis criteria for the high-resolution microendoscopic detection of neoplasia in Barrett's esophagus," J. Biomed. Opt. **15**, 026027 (2010).

19. K. Murari, Y. Zhang, S. Li, Y. Chen, M.-J. Li, and X. Li, "Compensation-free, all-fiber-optic, two-photon endomicroscopy at 1.55 μm," Opt. Lett. **36**, 1299–1301 (2011).

20. Y. Pu, L. Shi, S. Pratavieira, and R. Alfano, "Two-photon excitation microscopy using the second singlet state of fluorescent agents within the 'tissue optical window'," J. Appl. Phys. **114**, 153102 (2013).